ENERGY-BASED EVALUATION OF RC FRAME STRUCTURES

Mahyar Azizi[1], M. Altuğ Erberik[2]

[1] *Civil Eng. Department, Middle East Technical University, Ankara*
[2] *Prof. Dr., Civil Eng. Department, Middle East Technical University, Ankara*
Email: mhyrazizi@gmail.com

ABSTRACT:

Nowadays, earthquake and structural engineers perceive that conventional seismic design method, which is based on force and strength, is not an adequate way of designing structures underground motions. The reason is that the conventional seismic design method does not pay enough attention to inelastic displacements, plastic behavior of structures and duration of seismic motion. At the present time, there are new and popular alternatives to the force-based approach like displacement-based method, in which the aforementioned issues are mostly handled. Energy-based method is another convenient tool to study the performance of structures under seismic action and probably the best way to include duration of ground motion within the analysis. In energy based approach, the energy input to the structure should be dissipated through inelastic action and damping. The former energy dissipation mechanism is called as hysteretic energy. It is an important challenge to obtain the story-wise and component-wise distribution of the total hysteretic energy within the building in order to develop energy-based design and analysis tools. Accordingly, this study is focused on the story-wise and component-wise distribution of hysteretic energy in RC moment resisting frames. For this purpose, RC frames with different number of stories and bays are designed according to the 2018 Turkish Seismic Code. Then nonlinear time history (NLTH) analysis under 20 ground motion records are carried out and the distributions of hysteretic energy for each frame and analysis are obtained. The results indicate that it is possible to set up some rules for the hysteretic energy distribution in RC frames that can be used in energy-based design and analysis procedures.

KEYWORDS: energy-based design, hysteretic energy, RC frame, story-wise distribution, member-wise distribution, inelastic behavior, energy-based evaluation

1. INTRODUCTION

For the first time, Housner (1956) proposed the energy-based philosophy, which is based on the fact that the input energy of earthquake should be less than dissipation capacity of the structure. He presented a formula for input energy of SDOF systems. In the following years, many studies have been done to develop the energy-based design concept from SDOF systems to MDOF systems (McKevitt et al., 1980; Akiyama, 1985; Zhu et al., 1993; Shen and Akbas, 1999; Manfredi, 2001; Chou and Uang, 2003; Amiri et al., 2008).

In the energy-based approach, the input energy (E_i), which is representative of the intensity of the seismic action, is transmitted to the structure by kinetic energy (E_k), damping energy (E_d), elastic strain energy (E_s), and hysteretic energy (E_h). Kinetic energy represents the work done by inertia forces, and elastic strain energy is the stored energy in the form of elastic deformation. Damping energy reflects the dissipated energy by damping material. Hysteretic energy represents the dissipated input energy through cumulative plastic deformation, and it shows damage potential of the structure (Khashaee et al., 2003). Energy balance equation can be written as

$$E_i = E_k + E_d + E_s + E_h \quad (1)$$

Considering the inelastic behavior of the structure, E_k and E_s are very small compared to E_d and E_h during seismic action. It is possible to state that almost all the input energy of the earthquake is dissipated by damping energy and hysteretic energy at the end of the earthquake (Shen and Akbas, 1999).

$$E_i \cong E_d + E_h \tag{2}$$

Estimation of input energy is one of the most challenging parts of energy-based design philosophy. Surveying the previous literature about energy-based concept show that mostly, prediction of the input energy is the main focus. Hysteretic energy, which is another challenging part of the energy-based design concept, and in order to develop a practical energy-based design or assessment method, it is vital to estimate the hysteretic energy demand of structures and determine the distribution pattern of the hysteretic energy through the structure. However, estimation of hysteretic energy and its distribution in RC structures have been highlighted by a few studies (Guan and Du, 2013; Okur and Erberik, 2014; Tu and Zhao, 2018). There are also studies that focused on hysteretic energy in a detailed manner. However steel frames were used in these works (Uang and Bertero, 1990; Akbas et al., 2001; Leelataviwat et al., 2009; Akbas et al., 2016).

This study aims to carry out an energy-based evaluation on RC moment-resisting frames, with estimation of hysteretic energy and its story-wise and member-wise distribution. For this reason, RC moment-resisting frames with different numbers of stories and bays are selected, and their energy response under 20 ground motions are evaluated

2. CASE STUDY FRAMES

In this study 3, 5, 7, and 9 story RC moment resisting frame building models with different number of bays are selected. All span lengths of frames are taken as 6 meters from column centerlines, and all story heights are considered as 3 meters. Figure 1 shows the selected RC frame models, S where "S" is the reprehensive of story and "B"is the reprehensive of bay. For instance 3S-3B means 3-story, 3-bay frame.

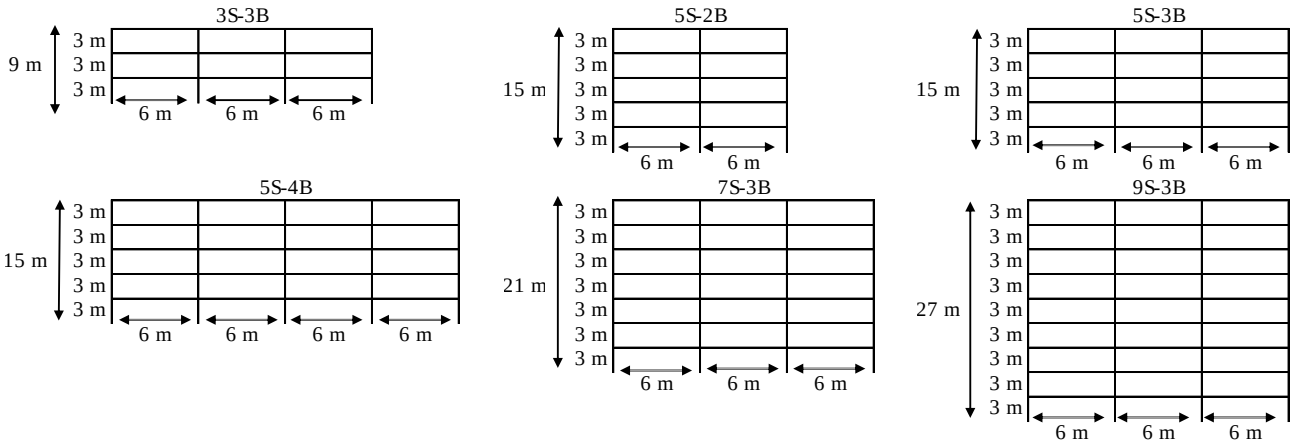

Figure 1. Selected moment-resisting RC frame models

The selected RC moment resisting frames are designed and detailed to satisfy requirements according to TS500 (Requirements for Design and Construction of Reinforced Concrete Structures) and TBSC 2018 (Turkish Building Seismic Code). In the design and analysis process, C25 for concrete and S420 for reinforcement is used. Applied gravity dead (G) and live load (Q) loads are selected, as stated in TS498 (Design Loads for Buildings). According to TS498 (1997), live load for residential buildings is selected as 2 kN/m^2. Flooring dead load is considered as 2

kN/m^2. Also, 3 kN/m wall weight load is applied to the beams directly. The live load reduction factors according to TS498 for residential buildings, are applied while designing frames.

For seismic design, peak ground acceleration (PGA) of 0.404g with a return period of 475 years is considered. According to TBDY (2018) Table 16.1, local soil class is assumed as ZD soil type which is composed of stiff clay and medium compact sand. Importance factor (I) and building usage class (BKS) are selected as 1 and 3, respectively, as stated in TBDY (2018) Table 3.1 for residential buildings. In order to investigate hysteretic behavior and energy dissipation of frames under earthquake, frames are designed as high ductile (A11) with structure system behavior factor (R) of 8 and over strength factor (D) of 3 according to Table 4.1 of the of TBDY. Horizontal elastic design spectrum is defined according to Chapter 2 of TBDY (2018).

Slab thickness is taken as 15 cm for all buildings. 15 cm thickness satisfies all strength and deflection requirements. All beams are considered as T-beam section, since it is assumed that RC beams and slabs are cast monolithically like typical residential buildings. Beam dimensions for selected frames are decided as 25 cm x 45 cm with 100 cm effective flange width. Column sections are square, and the section dimensions and reinforcements differ from story to story for all frames. Since the structures are chosen as high ductile moment resisting frames with R=8, strong column-weak beam check is also verified. According to the Turkish seismic code, in the beam-column joints, sum of the ultimate moment capacity of the columns shall be at least 20 % greater than the sum of ultimate moment capacity of the beams. Section dimensions and reinforcement details are summarized in Table 1.

Table 1. Member section design summary

Frame Type	Floor Number	Column size (cm)	Column Rebar	T-Beam Size(cm)	Beam Rebar	
					Top	Bottom
3 Story	1	35 x 35	8φ25	25 x 45	3φ18+6φ10	4φ16
	2	35 x 35	8φ25	25 x 45	3φ16+6φ10	3φ16
	3	35x 35	8φ20	25 x 45	3φ16+6φ10	3φ16
5 Story	1,2,3	50x50	12φ20	25 x 45	3φ18+6φ10	4φ16
	4,5	40 x 40	8φ25	25 x 45	3φ16+6φ10	3φ16
7 Story	1,2	60x60	16φ20	25 x 45	4φ18+6φ10	4φ16
	3,4,5	50x50	12φ20	25 x 45	4φ18+6φ10	4φ16
	6,7	40 x 40	8φ20	25 x 45	3φ16+6φ10	3φ16
9 Story	1,2	70 x 70	20φ20	25 x 45	4φ18+6φ10	4φ16
	3,4	60 x 60	16φ20	25 x 45	4φ18+6φ10	4φ16
	5	50 x 50	12φ20	25 x 45	4φ18+6φ10	4φ16
	6,7	50 x 50	12φ20	25 x 45	3φ18+6φ10	4φ16
	8,9	40 x 40	8φ20	25 x 45	3φ16+6φ10	3φ16

3. NLTH ANALYSIS

In order to investigate the energy-based seismic response of RC frame models under seismic action, nonlinear time history analysis is essential since it is possible to monitor the force-deformation relationship of all elements in each time step of ground motion record with NLTH analysis. SAP2000 (2017) structural analysis and design software is used for all linear and nonlinear analysis of this work.

3.1. Modeling

In this study, lumped plasticity model is used for NLTH analysis. In this modeling approach, nonlinear properties and moment-curvature relationship of the section are applied to the specific region of the element that is expected to go under plastic deformation. This plastic zone is called the plastic hinge. Usually, nonlinear properties of the plastic hinge are lumped at one or two nodes which are assumed to be constant within plastic hinge length (Lp), while plastic hinge and the rest of element has elastic section properties. Plastic hinge length has an integral role in the nonlinear models, and it affects deformation capacity of members. Plastic rotation of the plastic hinge could be calculated by multiplying plastic curvature with plastic hinge length. TBSC (2018) suggests that plastic hinge length should be equal to the half of the section depth (h) in the considered direction. This is a straightforward and practical assumption for the prediction of plastic hinge and it is used in this study for the sake of simplicity.

For NLTH analysis, the selected hinge could be capable of showing hysteresis behavior since hysteresis models make it possible to simulate the loading-unloading cycles and energy dissipation characteristics under time history of ground motions. Behavior of RC members and structures under cyclic loading is very complex, and a considerable number of studies and experiments has been done to find an analytical model to define realistic hysteretic behavior of RC members. In this study, hysteresis model proposed by Takeda et al (1970) is selected to simulate nonlinear behavior of RC frame. Takeda model has been used in many studies and it has been proven that it shows a reasonable response for flexural behavior of RC under cyclic loading.

3.2. Ground motion records

20 ground motions are selected for nonlinear time history analysis and energy calculations. These 20 ground motions are categorized into 2 groups as local and global ground motion records. Local ground motions are composed of 10 records from past earthquakes in Turkey, and global ground motions are composed of 10 records that were recorded in different locations around the world. In the selection of earthquakes, the main criterion is to have ground motion variability in terms of duration, intensity and frequency content. All ground motions are scaled for each case study RC frames according to the target design spectrum. The main characteristics of the selected ground motion records are presented in Table 2. In the second column of Table 2, a label is used for each ground motion record for the sake of simplicity. Local set of ground motions are labeled between L1 to L10 whereas global ground motions set are labeled between G1 to G10.

Table 2. Characteristics of the selected ground motion record

No	Label	Event	Country	Year	Location	Magnitude	PGA (g)	PGV (cm/s)
1	L1	Horasan	Turkey	1983	Horasan Meteorology Station	6.7	0.126	36.92
2	L2	Erzincan	Turkey	1992	Erzincan	7.3	0.469	92.05
3	L3	Dinar	Turkey	1995	Dinar Meteorology Station	6.1	0.319	40.61
4	L4	Marmara	Turkey	1999	Yarımca	7.8	0.322	79.60
5	L5	Marmara	Turkey	1999	Yarımca	7.8	0.230	84.70
6	L6	Marmara	Turkey	1999	Düzce	7.8	0.337	60.59
7	L7	Düzce	Turkey	1999	Düzce	7.3	0.410	65.76
8	L8	Düzce	Turkey	1999	Düzce	7.3	0.513	86.05
9	L9	Bingöl	Turkey	2003	Bingöl	6.400	0.509	34.48
10	L10	Ceyhan	Turkey	1998	Ceyhan	6.200	0.226	29.82
11	G1	Imperial Valley	USA	1979	El Centro Array #5, James Road	6.5	0.367	95.89
12	G2	Montenegro	Yugoslavia	1979	Ulcinj, Hotel Olimpic	7	0.241	47.08
13	G3	Loma Prieta	USA	1989	Hollister, South St. & Pine Dr.	7	0.369	62.78
14	G4	Manjil	Iran	1990	Abhar	7.3	0.209	55.44
15	G5	Cape Mendocino	USA	1992	Petrolia, General Store	7	0.662	89.45
16	G6	Northridge	USA	1994	Slymar, Converter Station	6.7	0.373	118.89
17	G7	Northridge	USA	1994	Jensen Filter Plant	6.7	0.424	106.22
18	G8	Kobe	Japan	1995	JMA	6.9	0.833	90.70
19	G9	Chi Chi	Taiwan	1999	TCU074, Nantou Nanguang School	7.6	0.595	74.64
20	G10	Tabas	Iran	1978	Tabas	7.3	0.241	47.08

4. ENERGY CALCULATIONS AND RESULTS

After NLTH analysis the energy parameters of the selected frame structures subjected to the given set of ground motion records are calculated. In order to contribute to the development of a practical energy-based design or assessment method, three primary steps are considered, which are: estimation of input energy, calculating the ratio of hysteretic energy to input energy (E_h/E_i) and evaluation of the distribution of hysteretic energy among stories and structural members. Estimation of the input energy is spotlighted by many studies while determination of the hysteretic energy of RC buildings has been taken into account in fewer previous work. Estimation of hysteretic energy and its distribution through stories and elements are the main focus of this study, and it is discussed in more detail.

4.1. Input energy results

Estimating the input energy of the earthquake is the first step in all the energy-based methods. . Housner (1956) and Akiyama (1985) proposed alternative approaches to predict the input energy for SDOF systems. Many studies have been carried out to extend the prediction of input energy from SDOF systems to MDOF systems (Shen and Akbas 1999, Manfredi 2001, Amiri et al. 2008, Okur and Erberik 2014, Alici and Sucuoglu 2018).
The input energy of each frame case is calculated for twenty ground motion records. The results are illustrated and compared to each other and the effect of ground motion characteristics and structural properties on input energy is discussed. Table 3 shows input energy per unit mass (E_i/m) of each ground motion for all frame models.

Table 3. E_i/m of 20 ground motions for all frame cases

E_i/m (cm/s)^2						
Ground motion	3-Story 3-Bay	5-Story 2-Bay	5-Story 3-Bay	5-Story 4-Bay	7-Story 3-Bay	9-Story 3-Bay
G1	771.0	650.4	680.6	694.6	1914.3	1341.7
G2	2315.6	736.2	723.4	713.2	378.3	325.0
G3	731.2	549.7	556.3	557.5	673.6	412.3
G4	3004.1	4265.9	4719.9	4930.0	4382.7	6208.9
G5	388.3	481.5	492.1	492.3	643.9	614.9
G6	1032.7	619.8	615.9	612.0	647.8	871.7
G7	1126.1	619.1	631.5	637.0	630.1	957.1
G8	473.2	674.0	670.4	664.9	475.3	622.3
G9	951.9	1062.4	1056.6	1046.7	360.9	672.8
G10	681.4	1356.6	1346.3	1336.2	843.7	602.1
L1	11990.1	1879.1	2063.7	2163.5	1837.0	2461.8
L2	576.3	498.0	507.3	511.3	975.1	536.9
L3	2499.2	913.3	908.1	902.8	795.1	533.8
L4	1517.4	1082.6	1104.6	1105.2	369.5	1374.9
L5	824.6	1060.4	1107.4	1135.0	1916.8	1719.9
L6	808.0	1163.1	1202.6	1223.3	1267.9	1136.0
L7	1126.1	1468.8	1510.8	1524.0	1172.2	1207.8
L8	597.2	1158.6	1173.9	1177.6	615.7	714.1
L9	808.2	2226.5	2218.3	2205.1	1062.5	751.9
L10	1065.1	617.6	609.6	604.6	3960.0	2935.5

Comparing the input energies of all ground motions for all moment-resisting frames, it can be stated that although all ground motions are scaled to the equivalent spectral acceleration, the energies of different ground motion records have totally different values. Input energy also seems to be period-dependent. This means that input energy is dependent on both ground motion characteristics and structural properties.

Table 3 shows that G4 (Manjil 1990) record gives the highest amount of input energy for 5-story,7-story and 9-story frame models. For the 3-story frame model, G4 record yields the second-highest input energy value after L1 record. PGA and PGV values of the G4 record is 0.21 g and 47.1 cm/s, respectively, which are not high compared to L2, L7, L8 and G8 records (Table 2). However Figure 2 shows that G4 record has a long duration with many high amplitude acceleration cycles. It is possible to conclude that PGA and PGV are not adequate ground motion parameters for the representation of earthquake damage potential and other ground motion characteristics like duration and number of high amplitude acceleration cycles should be taken into account.

Also the results show that input energy is almost constant among 5 story frames and it shows that each ground motion record gives similar values of input energies for 5-Story 2-Bay. 5-Story 3-Bay and 5-Story 4-Bay frames. This is expected because all 5 story frames with different bay numbers have similar fundamental periods and damping ratios. So, the fundamental period is an important parameter, and a ground motion record applies nearly the same input energy to different structures with similar fundamental periods and damping ratios although geometrical properties (like number of bays) may differ.

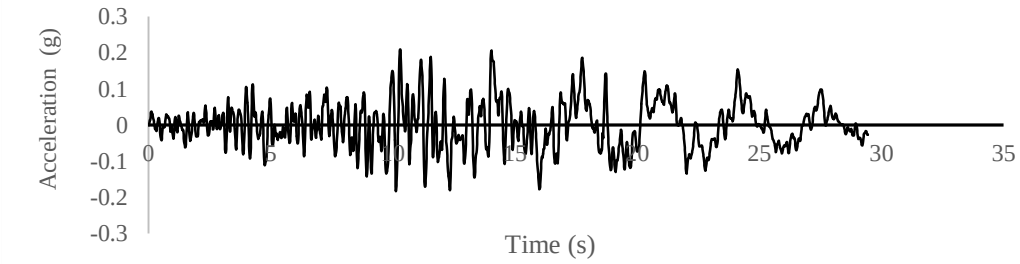

Figure 2. G4 (Manjil 1990) ground motion record.

4.2. The Ratio of Hysteretic to Input Energy:

In order to propose a practical energy-based design or evaluation methodology, hysteretic energy, which is the representative of the damage potential of the structure, should be predictable. Fajfar et al. (1990) stated that it is possible to predict hysteretic energy demand using the ratio of hysteretic to input energy.

E_h/E_i and E_d/E_i ratios of all frame models under 20 ground motion records are calculated as presented in Table 4. Mean values and coefficient of variation percentages (COV%) of the ratios also illustrated in the last two rows of the table. In order to observe the effect of ground motion characteristics and structural properties on hysteretic energy, the percentage of E_h/E_i ratio for all ground motions are plotted for each frame model in Figure 3.

Table 4. E_d/E_i and E_h/E_d ratios of all ground motion records for all frame models

Ground motion labels	3-Story, 3-Bay		5-Story, 2-Bay		5-Story, 3-Bay		5-Story, 4-Bay		7-Story, 3-Bay		9-Story, 3-Bay	
	Eh/Ei	Ed/Ei	Eh/Ei	Ed/Ei	Eh/Ei	Ed/Ei	Eh/Ei	Ed/Ei	Eh/Ei	Ed/Ei	Eh/Ei	Ed/Ei
G1	0.68	0.31	0.67	0.31	0.67	0.31	0.66	0.31	0.63	0.37	0.62	0.38
G2	0.63	0.37	0.61	0.37	0.61	0.37	0.61	0.37	0.56	0.44	0.53	0.46
G3	0.62	0.36	0.58	0.40	0.58	0.40	0.58	0.40	0.56	0.43	0.54	0.46
G4	0.69	0.31	0.67	0.32	0.67	0.33	0.67	0.33	0.65	0.35	0.58	0.41
G5	0.57	0.40	0.59	0.38	0.59	0.38	0.59	0.38	0.56	0.44	0.53	0.46
G6	0.66	0.33	0.61	0.37	0.61	0.37	0.61	0.37	0.60	0.40	0.60	0.40
G7	0.65	0.34	0.63	0.35	0.63	0.35	0.63	0.35	0.63	0.37	0.60	0.40
G8	0.58	0.39	0.55	0.44	0.54	0.44	0.54	0.44	0.51	0.49	0.47	0.53
G9	0.58	0.41	0.56	0.43	0.56	0.43	0.56	0.43	0.48	0.51	0.51	0.49
G10	0.54	0.45	0.59	0.40	0.58	0.41	0.58	0.41	0.55	0.45	0.51	0.49
L1	0.57	0.42	0.70	0.30	0.69	0.30	0.69	0.30	0.67	0.32	0.62	0.38
L2	0.63	0.35	0.61	0.37	0.61	0.36	0.61	0.36	0.60	0.40	0.58	0.42
L3	0.63	0.37	0.57	0.41	0.57	0.41	0.57	0.41	0.55	0.44	0.53	0.47
L4	0.66	0.33	0.64	0.35	0.64	0.34	0.65	0.34	0.57	0.43	0.62	0.38
L5	0.62	0.36	0.63	0.35	0.64	0.35	0.64	0.35	0.66	0.33	0.66	0.34
L6	0.62	0.37	0.63	0.35	0.63	0.35	0.63	0.35	0.63	0.36	0.61	0.38
L7	0.65	0.34	0.57	0.42	0.58	0.41	0.58	0.41	0.58	0.41	0.58	0.41
L8	0.59	0.39	0.61	0.38	0.61	0.38	0.61	0.38	0.58	0.42	0.59	0.41
L9	0.52	0.47	0.52	0.47	0.52	0.47	0.52	0.47	0.52	0.48	0.50	0.50
L10	0.56	0.42	0.49	0.49	0.49	0.49	0.49	0.49	0.54	0.46	0.53	0.47
Mean	0.61	0.37	0.60	0.38	0.60	0.38	0.60	0.38	0.58	0.41	0.57	0.43
Cov %	7.48	11.65	8.26	12.84	8.16	12.60	8.07	12.50	8.59	12.33	8.76	11.68

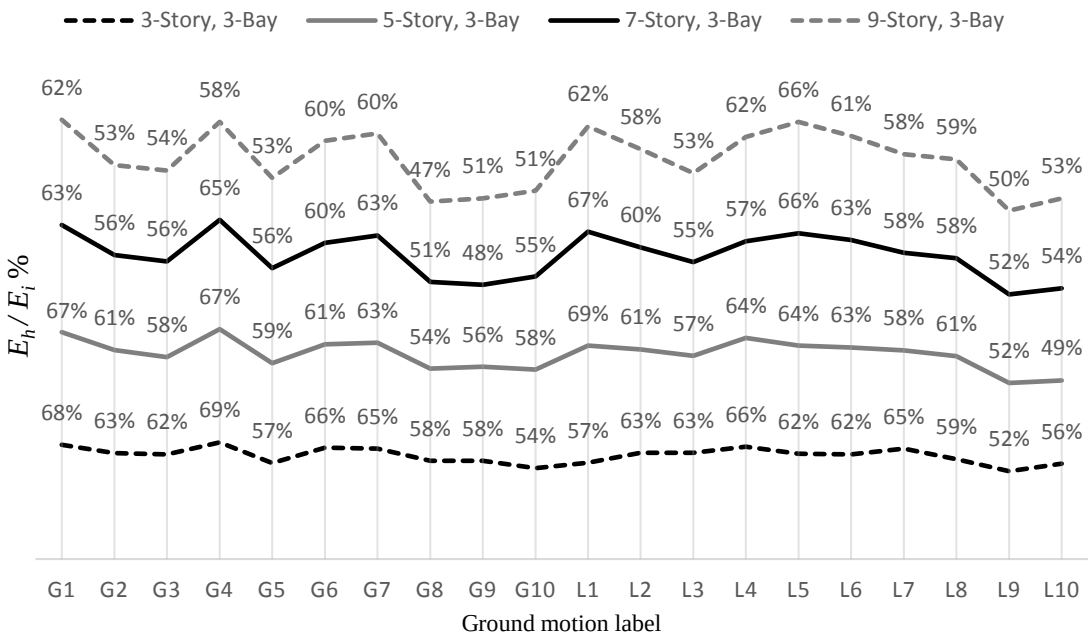

Figure 3. Comparison of the E_h/E_i ratio shown as percentage for each frame model for all ground motion records

Table 4 verify that these two mechanisms of energy dissipation should be equal to the energy imparted to the structure at the end of the ground motion record. The results show that Percentage of hysteretic to input energy ratio varies from 48% to 70% where the mean value of the E_h/E_i ratio for 20 ground motion records for the 3-story frame is 0.61, for the 5-story frame is 0.60, for the 7-story is 0.58 and for the 9-story frame is 0.57. The percentage of coefficient of variation is about 8% which means that the level of dispersion around the mean is low. According to the results of this study it could be concluded that for an RC moment-resisting frame that exhibits inelastic behavior, almost 60% of the input energy is dissipated through hysteretic action and 40% is dissipated through damping action.

Comparing E_h/E_i ratio of all ground motions for each frame model in Figure 3 shows that E_h/E_i ratio line is nearly constant for 3 story frame and as the number of stories increases the ratio line become more sensitive to the ground motion. This means that as the fundamental period of structure increases, E_h/E_i ratio becomes more dependent on ground motion characteristics.

The values on the vertical grid-lines in Figure 3 show the variation of the E_h/E_i ratios with respect to frame models for the same ground motion record. Looking from this perspective it can be stated that there is a slight dependence of E_h/E_i ratio to the selected frame model. However this slight dependence can be ignored for the sake of simplicity to develop simple and practical design procedures.
To sum up, hysteretic demand and E_h/E_i ratio are dependent on both structural properties and ground motion characteristics. This dependence seems to be more pronounced for ground motion characteristics compared to the structural properties for the considered data set.

4.3. Distribution of Hysteretic Energy

It is necessary to know how the hysteretic energy is distributed within the stories and structural elements, in order to develop energy-based design and assessment methodologies. For this reason, the hysteretic energies of all plastic hinges of the selected 6 moment-resisting frames under 20 ground motion have been calculated and the results of hysteretic energy distribution are illustrated. The results are presented in terms of story-wise and member-wise distribution of hysteretic energy.

4.3.1. Story-wise Distribution of the Hysteretic Energy

Hysteretic energy dissipated at the column and beam hinges are summed in each story and divided by the total hysteretic energy of the frame to find the cumulative hysteretic energy demand of each story. The distribution of story-wise hysteretic energy to total hysteretic energy ratio (E_{sh}/E_h) over the height of the structures for different ground motion record are shown for global ground motion set in Figure 4 and Figure 5 in which MG represent mean value of the results for global records**.**

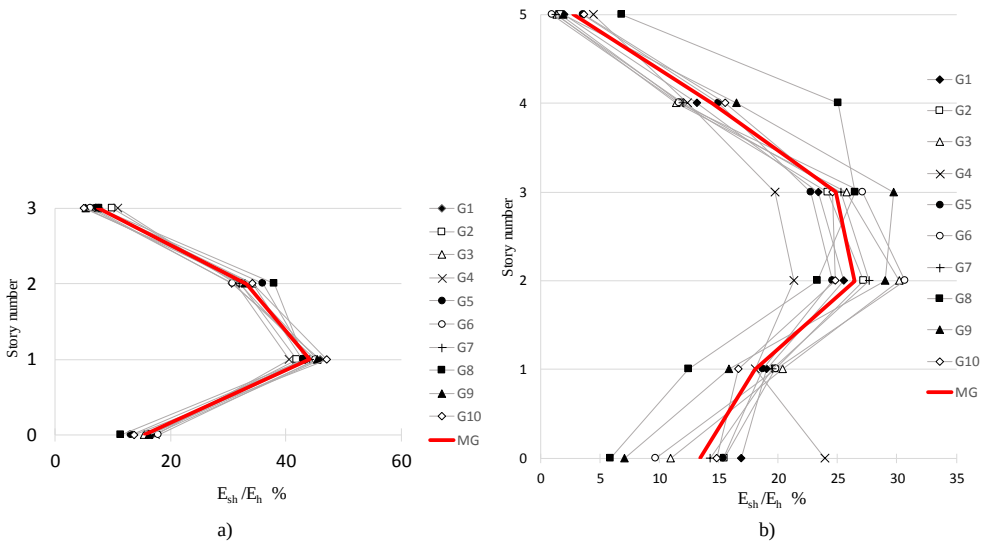

Figure 4. E_{sh}/E_h % for a) 3S-3B frame b) 5S-3B frame

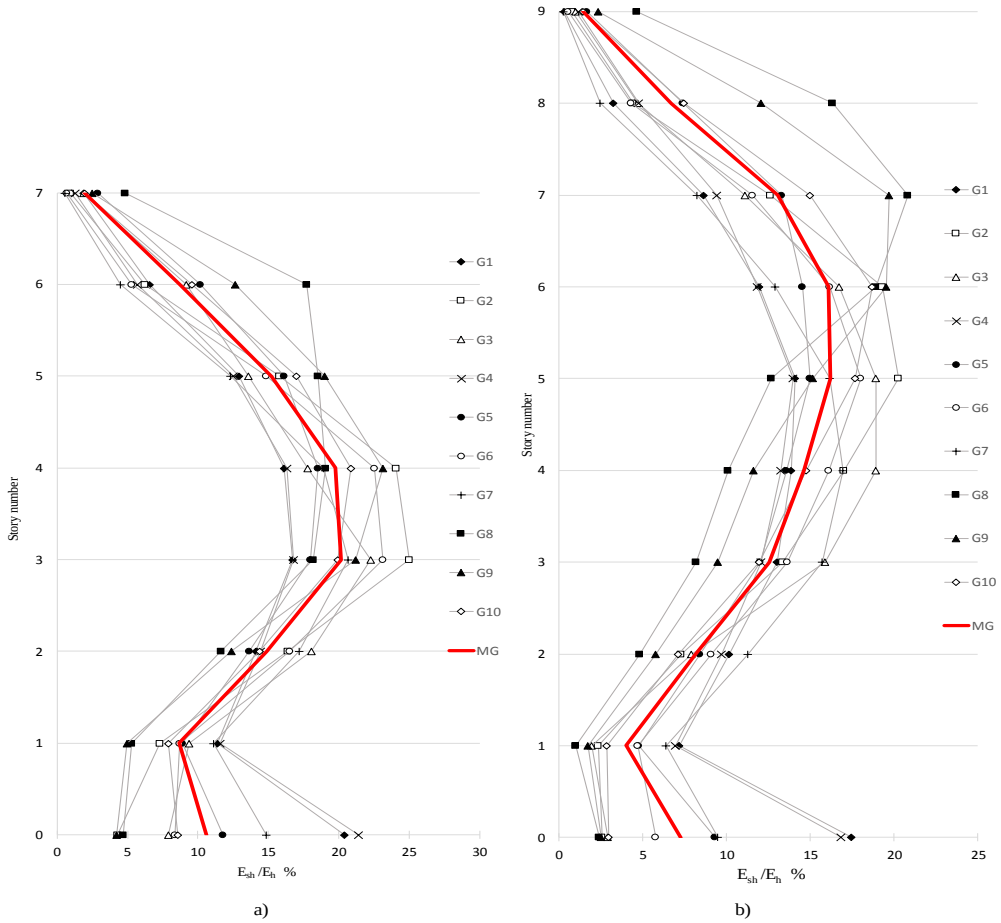

Figure 5. E_{sh}/E_h % for a) 7S-3B frame b) 9S-3B frame

General trend of the results show that distribution of hysteretic energy over the height of structure depends on both ground motion characteristics and structural properties. For 3 story frame, E_{sh}/E_h ratios for all ground motions are close to each other whereas, the ratio values have more scatter for other frame models. This shows that story-wise distribution of hysteretic energy is less sensitive to ground motion characteristics for low-rise buildings. The results show that about 75% of the hysteretic energy is dissipated in the second and third story for 3 story frame. This percentage decreases to 45% for the 5 story frame model, 25% for the 7 story frame model and 15% for the 9 story frame model. In addition, the dissipated hysteretic energy by the base columns decreases from 15% for the 3 story frame to 9% for the 9 story frame. It means that as the fundamental period of the structure increases as hysteretic energy moves from the lower stories to the mid and upper stories.

4.3.2. Member-wise Distribution of Hysteretic Energy

The dissipated hysteretic energy at each beam and column hinge is divided by the total hysteretic energy to obtain the ratio of member-wise (beam or column) hysteretic energy to total hysteretic energy (E_{mh}/E_h) for all ground motions as a measure. Total hysteretic energy percentage dissipated by the base columns (sum of E_{mh}/E_h% at base columns), story columns (sum of E_{mh}/E_h% at story columns) and story beams (sum of E_{mh}/E_h% at story beams) for all records are calculated and the mean values of them are presented in Table 5. The member sections were designed considering strong column-weak beam criterion. So, it is expected that most of the hysteretic energy is dissipated by beam members

In order to have a deeper perception about the member-wise distribution of hysteretic energy, mean values of E_{mh}/E_h % at each plastic hinge for two record sets are illustrated in Figures 5.25-5.30. This contributes to compare the hysteretic energy demand of all beam or column hinges in the same story.

Table 5. Mean values of hysteretic energy dissipated percentage by beam and column members for 10 global and local records

Frame case	Ground motion set	Structural Element		
		Base Columns	Story Columns	Beams
3S-3B frame	Global set	15.4	16.4	68.2
	Loal set	14.3	18.9	66.8
5S-2B frame	Global set	12.8	5.7	81.6
	Loal set	14.2	6.5	79.3
5S-3B frame	Global set	13.4	5.9	80.7
	Loal set	15.1	7.0	77.9
5S-4B frame	Global set	13.9	6.1	80.1
	Loal set	15.5	7.2	77.3
7S-3B frame	Global set	10.6	8.3	81.0
	Loal set	13.3	8.7	78.0
9S-3B frame	Global set	7.2	7.7	85.1
	Loal set	10.0	7.0	83.0

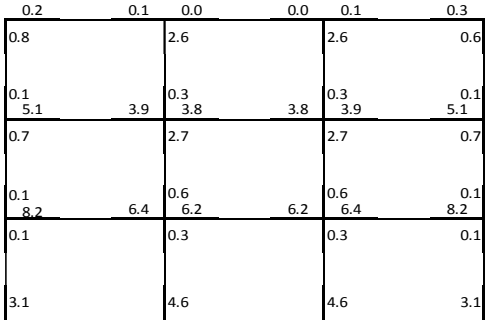

Figure 5. Mean values of E_{mh}/E_h at of 7S-3B frame

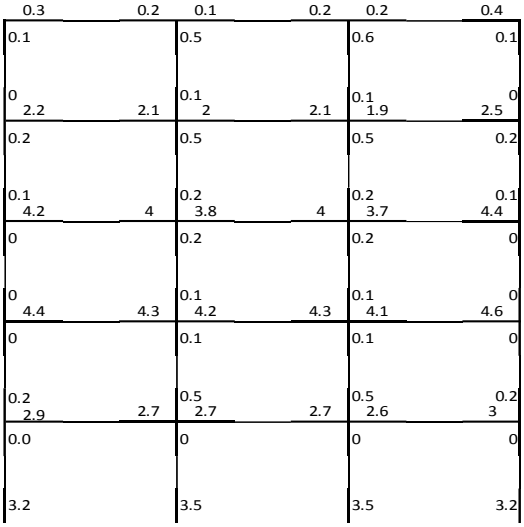

Figure 6. Mean values of E_{mh}/E_h at of 7S-3B frame

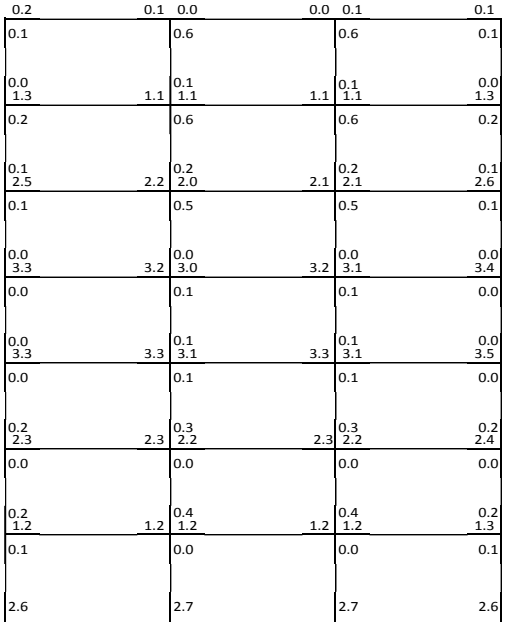

Figure 7. Mean values of E_{mh}/E_h at of 7S-3B frame l

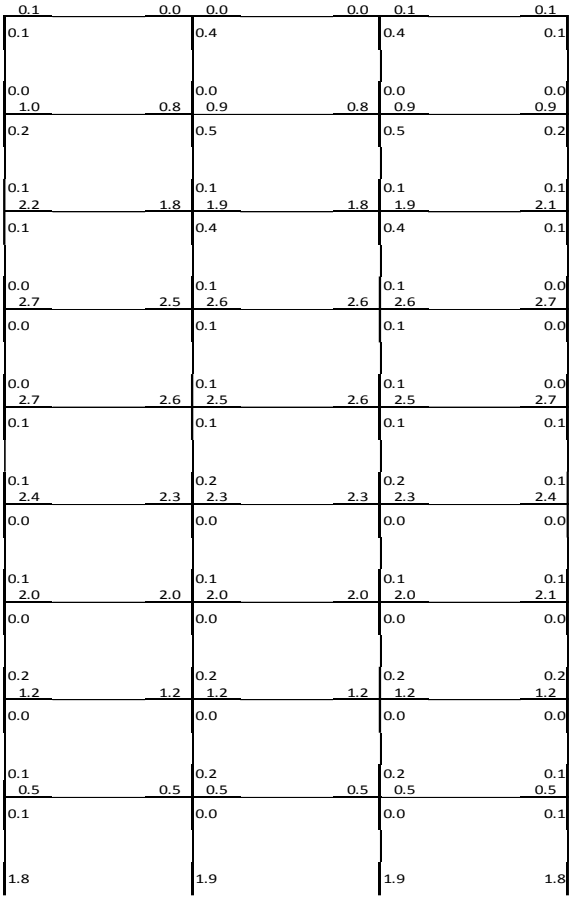

Figure 8. Mean values of E_{mh}/E_h at of 9S-3B frame

Calculated mean values of hysteretic energy dissipated by column and beam hinges for all analysis cases shows that 78% of total hysteretic energy is dissipated by beam hinges whereas 9% is dissipated by column hinges in the stories and 13% is dissipated by the hinges at the base columns. It seems that the ratio of dissipated hysteretic energy by columns to dissipated hysteretic energy by beams is sensitive to the ultimate moment capacities of column and beam sections. Although the column moment capacity to beam moment capacity ratio is more than 1.2 for all frame models, columns did not stay in the elastic zone, and they showed hysteretic behavior. It could be concluded that the 1.2 ratio that mentioned in many codes, does not guarantee the elastic behavior of columns and it causes a ductile beam-column failure mechanism. From Table 5, it is observed that as fundamental period of the structure increases, dissipated hysteretic energy from base columns is transferred to the beams.

Comparing E_{mh}/E_h ratios from Figures 7-8, shows that the hysteretic energy is distributed equally between interior members and also it is distributed equally between exterior members (here beams are compared together and columns are compared together). However the percentage of hysteretic energy dissipated by exterior and interior members are not always the same. E_{mh}/E_h ratios for exterior beam hinges are greater than the E_{mh}/E_h ratios for interior beam hinges. The inverse of this occurs for columns and the E_{mh}/E_h ratios for exterior column hinges are less than the E_{mh}/E_h ratios for interior columns hinges. This means that the hysteretic energy demand of exterior beams and interior columns are more than the hysteretic energy demand of the interior beams and exterior columns of the same story in RC moment-resisting frames.

Finding the difference of E_{mh}/E_h ratios between exterior and interior beam hinges for all stories and taking their average, show that hysteretic energy dissipated by exterior beam hinges is 30% more than the hysteretic energy dissipated by the interior beam hinges for 3 story frame, 15 % for 5 story frame, 8% for 7 story frame and 4% for 9 story frame. This means that as fundamental period of the structure increases the difference of of E_{mh}/E_h ratios between exterior and interior beam hinges decreases. Since, the hysteretic energy dissipated by columns are slight and majority of the energy is dissipated by beams, it is possible to ignore the difference of E_{mh}/E_h ratios between exterior and interior column hinges.

To sum up, member-wise distribution of hysteretic energy is directly influenced by the moment capacities of beam and column sections whereas the dependence is slight for ground motion characteristics. This shows that it is possible to propose practical energy-based design rules to control the distribution of inelastic action within a frame structure.

5. Summary and Conclusions

This study aims to evaluate the energy-based response of RC moment-resisting frames designed according to TBSC 2018. Since most of the previous studies have concentrated on the input energy, the main focus of this study is on the estimation of hysteretic energy and its story-wise and member-wise distribution. For this reason, 6 RC moment-resisting frames with different number of stories and bays are selected and designed according to TBSC 2018. Then, NLTH analyses are carried out under 20 selected strong ground motion records. Energy parameters of the frame models are calculated in terms of E_i and E_h/E_i. The obtained results are examined to understand the effect of ground motion characteristics and structural properties on E_i and propose a practical value for E_h/E_i ratio to estimate hysteretic energy demand. In last part of the study, hysteretic energy dissipated by each plastic hinge in the frame models is calculated to obtain the story-wise and member-wise distribution of hysteretic energy. The final results show that it is possible to propose a methodology to determine hysteretic demand of each story and member of a well-designed RC frame under seismic action.

The main results of this study can be summaries as follow

- Input energy depends on both structural properties and ground motion characteristics.
- For energy-based design or assessment purposes, a constant value of 0.7 can be suggested for the E_h/E_i ratio.
- The dependency of the E_{sh}/E_h ratio to ground motion characteristics becomes more obvious as fundamental period of structure increases.
- The second mode of the structures should be considered in an energy-based design or assessment methodology, especially for mid-rise and high-rise RC frames.
- In general terms, 70%-85% of the energy is dissipated by beams, 8%-18% by story columns and 7%-15% by base columns (the percent depends on the capacity ratio)
- Strong column-weak beam criterion does not guarantee elastic behavior for columns.
- Hysteretic energy is generally distributed uniformly among the interior members (the trend is also the same for exterior members).
- Hysteretic energy demands of exterior beam hinges are generally more than interior beam hinges (the trend is just the opposite for columns).
- As number of stories and fundamental period of structure increase, hysteretic energy is distributed more uniformly in the same story.
- It seems it is possible to propose a practical energy-based methodology (further studies are needed).

REFERENCES

Akiyama, H. (1985). Earthquake-resistant limit-state design for buildings. University of Tokyo Press.

Alıcı, F. S., & Sucuoğlu, H. (2018). Elastic and inelastic near-fault input energy spectra. Earthquake Spectra, 34(2), 611-637.

Amiri, J. V., Amiri, G., & Ganjavi, B. (2008). Seismic vulnerability assessment of multi-degree-of-freedom systems based on total input energy and momentary input energy responses. Canadian Journal of Civil Engineering, 35(1), 41-56.

Chou, C. C., & Uang, C. M. (2003). A procedure for evaluating seismic energy demand of framed structures. Earthquake Engineering & Structural Dynamics, 32(2), 229-244.

CSI (2017). CSI Analysis Reference Manual for SAP200, ETABS, and SAFE. Computers and Structures, Inc. Berkeley, California.

CSI (2018). SAP2000 Version 20.1.0, Linear and Nonlinear Static and Dynamic Analysis and Design of Three Dimensional Structures: Basic Analysis Reference Manual. Computers and Structures, Inc. Berkeley, California.

Fajfar, P., Vidic, T., & Fischinger, M. (1990). A measure of earthquake motion capacity to damage medium-period structures. Soil Dynamics and Earthquake Engineering, 9(5), 236-242.

Guan, M., & Du, H. (2013). Energy-based seismic performance of reinforced concrete frame structures. Magazine of Concrete Research, 65(8), 494-505

Housner, G. W. (1956). Limit design of structures to resist earthquakes. In Proc. of 1st WCEE (pp. 5-1).

Kalkan, E., & Kunnath, S. K. (2008). Relevance of absolute and relative energy content in seismic evaluation of structures. Advances in Structural Engineering, 11(1), 17-34.

Khashaee, P., Gross, J. L., Khashaee, P., Lew, H. S., Mohraz, B., & Sadek, F. (2003). Distribution of earthquake input energy in structures (pp. 1-36). US Department of Commerce, National Institute of Standards and Technology.

Manfredi, G. (2001). Evaluation of seismic energy demand. Earthquake engineering & structural dynamics, 30(4), 485-499.

Massumi, A., & Monavari, B. (2013). Energy based procedure to obtain target displacement of reinforced concrete structures. Structural Engineering and Mechanics, 48(5), 681-695.

McKevitt, W. E., Anderson, D. L., & Cherry, S. (1980). Hysteretic energy spectra in seismic design. In Proceeding of the Seventh World Conference on Earthquake Engineering (pp. 487-494)

Merter, O., & Ucar, T. (2014). Design of RC frames for pre-selected collapse mechanism and target displacement using energy–balance. Sadhana, 39(3), 637-657.

Okur, A., & Erberik, M. A. (2014, August). Adaptation of Energy Principles in Seismic Design of Turkish RC Frame Structures. Part II: Distribution of Hysteretic Energy. In Proceedings of the 2nd European Conference on Earthquake Engineering and Seismology, August (pp. 25-29).

Shen, J., & Akbaş, B. (1999). Seismic energy demand in steel moment frames. Journal of Earthquake Engineering, 3(04), 519-559.

Tu, B. B., & Zhao, D. (2018). Distribution of accumulated irrecoverable hysteretic energy in MDOF structures. Multidiscipline Modeling in Materials and Structures, 14(2), 202-215.

Turkish Earthquake Code, TEC (2007) Specifications for the buildings to be constructed in disaster areas. Ministry of Public Works and Settlement, Ankara, Turkey

Turkish Building Earthquake Code, TBEC (2018) Republic of Turkey Prime Ministry Disaster and Emergency Management Authority, Ankara, Turkey

Turkish Standard Institute (1997). Turkish Standard, TS498: The Calculation Values of Loads used in Designing Structural Elements. Ankara, Turkey, 21 p

Turkish Standards Institute (2000). Turkish Standard, TS500: Requirements for design and construction of reinforced concrete structures. Ankara, Turkey

Zhu TJ ,Tso WK, Heidebrecht HC.(1993). Seismic energy demands on reinforced concrete moment- resisting frames. Earthquake Engineering and Structural Dynamics 1993; 22(5):533–545